The Generation of Barotropic Edge Waves by Deep-Sea Internal Waves[1]

DAVID C. CHAPMAN

Woods Hole Oceanographic Institution, Woods Hole, MA 02543

(Manuscript received 17 February 1984, in final form 6 April 1984)

ABSTRACT

A simple two-layer, step-shelf model is used to demonstrate that barotropic (surface) edge waves of substantial amplitude can, in principle, be generated by deep-sea internal waves incident upon the coastal topography. Some qualitative features of the results suggest that this mechanism could account for the edge-wave "noise" observed by Munk and others.

1. Introduction

Barotropic edge waves are super-inertial surface gravity waves which are trapped at a coastline and propagate freely along the coastline in either direction. They are refractively trapped in the sense that the trapping depends on the offshore depth increase and not, for example, on the earth's rotation. For any monotonically increasing depth profile, there is, in principle, an infinite set of possible discrete edge-wave modes, each of which has a different number of zero-crossings in its offshore structure. Further, the edge-wave frequencies increase with mode number (at constant alongshelf wavenumber) and with alongshelf wavenumber for a particular mode (see Huthnance, 1975, for details).

Edge waves have been observed along a number of coastlines over a wide range of frequencies. For example, recent observations of surf beat (Huntley *et al.*, 1981) suggest that much of the energy is in the form of progressive edge waves. At these frequencies [15–60 cycles per hour (cph)], the edge waves are trapped fairly close to shore (within about 200 m) and may be important in many nearshore processes. Evidence from both theoretical and laboratory studies (e.g., Bowen and Guza, 1978) suggests that these edge waves may be generated by the nonlinear transfer of energy from incident surface waves to the edge waves.

At lower frequencies (3–10 cph), the offshore trapping scale is larger (2–20 km), and edge waves can apparently be generated by the passage of storm systems over the continental shelf (e.g., Munk *et al.*, 1956; Beardsley *et al.*, 1977). However, some edge-wave energy at these frequencies has been observed to persist considerably longer than storm time scales (Munk *et al.*, 1956, 1964). Such edge waves have relatively small amplitudes (~1 cm of sea-surface elevation; dubbed edge-wave "noise" by Munk *et al.*, 1956), but they show remarkable agreement with theory in that the spectral peaks in frequency–alongshelf wavenumber space occur very close to the predicted dispersion curves (e.g., Munk *et al.*, 1964, Fig. 10). In this case, the lowest-mode edge wave was most highly excited and the edge-wave energy decreased with increasing frequency. The generating mechanism for the edge-wave "noise" is still unclear, and a model of atmospherically forced edge waves (Buchwald and de Szoeke, 1973) suggests that some other mechanism must account, at least in part, for these persistent edge waves.

The purpose of this paper is to suggest that edge-wave "noise" could be the result of deep-sea internal waves impinging upon coastal topography. One appealing aspect of this idea is that deep-sea internal waves, unlike the atmosphere, represent a relatively constant energy source for the edge-wave "noise." Another favorable aspect is that the observed edge waves were found to have nearly equal energy traveling in both directions, and their phases appeared random (Munk *et al.*, 1964). These features would be expected if the energy source were horizontally isotropic, e.g., the deep-sea internal-wave field. The intent is merely to demonstrate the feasibility of the mechanism and not to make quantitative comparisons with observations. Thus, only the simple two-layer model shown in Fig. 1 will be considered (Section 2), the near-resonant behavior of which is detailed in Section 3, followed by a summary in Section 4.

The model also serves another purpose. In a linear, two-layer, inviscid ocean with a flat bottom, baroclinic and barotropic modes are uncoupled. In the presence of bottom topography, order-one barotropic motions can produce large baroclinic motions, as in the generation of internal tides (e.g., Rattray, 1960). The reverse is not typical and has led to the development

[1] Woods Hole Oceanographic Institution Contribution No. 5579.

of approximate models which treat the baroclinic mode of a two-layer ocean alone when the bottom is not flat (e.g., Cushman-Roisin and O'Brien, 1983). However, the present model shows that, in coastal regions, order-one baroclinic motions can produce large barotropic motions. Romea and Allen (1982), using an exponential shelf-slope, found similar strong coupling between baroclinic and barotropic motions at subinertial frequencies which produced large-amplitude barotropic shelf waves. Further, since virtually any coastal topography can support edge waves and shelf waves, these results should apply to other topographies as well. Thus, an *a priori* assumption of negligible barotropic response to baroclinic motions over variable bottom relief should be made with great caution.

2. A simple model

To demonstrate the generation of barotropic edge waves by deep-ocean internal waves, I consider the simple model depicted in Fig. 1. The deep ocean is stably stratified with two immiscible fluids with slightly different densities. The upper layer has mean thickness H_1 and density ρ, while the lower layer has thickness $H_2 = H - H_1$ and density $\rho(1 + \epsilon)$, where $\epsilon \ll 1$. The deep ocean borders a step shelf having width L, constant depth d and containing homogeneous fluid of density ρ. Thus, the interface depth H_1 is always greater than the shelf depth d. Rotation effects are neglected and motions are assumed linear. The problem consists of determining the response of the free-surface displacement η over the shelf to an internal gravity wave (on the interface ζ) incident from the deep ocean ($x = \infty$). (Mysak, 1968, has considered the effects of stratification on edge waves using a two-layer model, but he viewed stratification as a dissipative mechanism and did not consider any generation mechanisms.)

The wavelengths of both surface and internal waves are assumed long, compared to the water depth, so

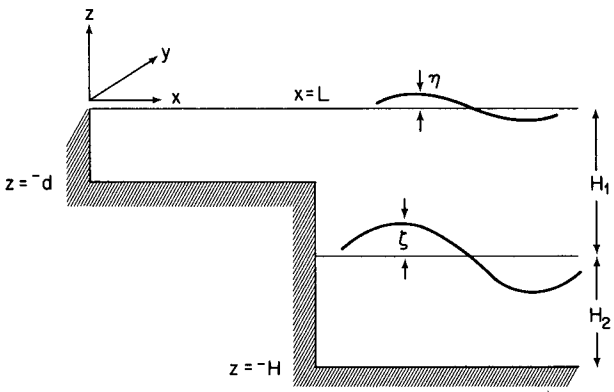

FIG. 1. Step-shelf model with two-layer stratification in the deep-sea region.

that the shallow water (hydrostatic) approximation may be made. This assumption has been shown to have negligible effect on edge waves in a homogeneous fluid over a step shelf (Miles, 1981), so it is expected to have little effect in the two-layer case as well. The appropriate equations of motion for a nonrotating, two-layer fluid are

$$u_t^u = -g\eta_x, \tag{1a}$$

$$v_t^u = -g\eta_y, \tag{1b}$$

$$(u_x^u + v_y^u)H_1 + \eta_t - \zeta_t = 0, \tag{1c}$$

$$u_t^L = -g[(1 - \epsilon)\eta_x + \epsilon\zeta_x], \tag{2a}$$

$$v_t^L = -g[(1 - \epsilon)\eta_y + \epsilon\zeta_y], \tag{2b}$$

$$(u_x^L + v_y^L)H_2 + \zeta_t = 0, \tag{2c}$$

where (u^u, v^u) and (u^L, v^L) are the cross-shelf (x) and alongshelf (y) velocities in the upper and lower layers, respectively, and g is gravitational acceleration. Subscripts x, y, t denote partial differentiation.

For simplicity, variables are scaled as follows:

$$\begin{aligned} x, y &\text{ by } L, \\ d, H_1, H_2 &\text{ by } H, \\ u^u, v^u, u^L, v^L &\text{ by } U, \\ \eta, \zeta &\text{ by } U(H/g)^{1/2}, \\ t &\text{ by } L/(gH)^{1/2}, \end{aligned}$$

where U is a typical velocity. Motions are also assumed monochromatic and propagating in the alongshelf direction with frequency ω and wavenumber l, i.e., $\propto \exp(i\omega t \pm ily)$. The problem is solved by first finding appropriate solutions for the shelf region and for the deep ocean separately, and then requiring continuity of surface displacement and normal mass transport at the shelf break ($x = 1$). Note that, with the above scaling, the deep ocean has unit depth.

Deep-ocean solutions are found by combining (1) and (2) into a single equation for the deep-ocean surface displacement (in scaled form),

$$\left(\frac{\partial^2}{\partial x^2} - \beta_+^2\right)\left(\frac{\partial^2}{\partial x^2} + \beta_-^2\right)\eta^D = 0, \tag{3}$$

where

$$\beta_+^2 = \left(l^2 - \frac{\omega^2}{c_+^2}\right), \quad \beta_-^2 = \left(\frac{\omega^2}{c_-^2} - l^2\right),$$

$$c_\pm^2 = \frac{1}{2} \pm \frac{1}{2}(1 - 4\epsilon H_1 H_2)^{1/2}.$$

An appropriate solution of (3) is

$$\eta^D = Ie^{i\beta_-(x-1)} + Be^{-i\beta_-(x-1)} + Ce^{-\beta_+(x-1)}, \tag{4}$$

where the unknown (complex) coefficients (I, B, C) represent the contributions to the surface displacement

due to the incident internal wave, the reflected internal wave, and the exponentially decaying surface wave, respectively. Note that (3) and (4) are written such that $lc_- < \omega < lc_+$ results in real β_+, β_-; i.e., the surface wave decays exponentially offshore as in the case of an edge wave, while the internal wave is periodic (i.e., propagating) offshore. Note also that for appropriate ω and realistically small ϵ, $\beta_- \gg l$ which means that the internal wave is almost normally incident upon the shelf [the angle of incidence from normal being given by $\tan^{-1}(l/\beta_-)$].

It is simplest to consider an internal wave of unit interface displacement which contributes a surface displacement of

$$I = \mu^{-1} = \left(1 - \frac{H_1}{c_-^2}\right)^{-1} \tag{5}$$

(Gill, 1982, p. 120). Using this value of I [an $O(\epsilon)$ quantity], the total surface displacement over the shelf or deep ocean represents the response due to an incident internal gravity wave with unit interface displacement.

Motions in the homogeneous fluid over the shelf are described by (1) with $\zeta = 0$ and H_1 replaced by d in (1c). Combining this form of (1) into a single equation for the surface displacement over the shelf leads to (in scaled form)

$$\left(\frac{\partial^2}{\partial x^2} + \alpha^2\right)\eta^S = 0, \tag{6}$$

where $\alpha^2 = (\omega^2/d) - l^2$. An appropriate solution of (6) which satisfies the boundary condition of no flow through the coast ($u = 0$ at $x = 0$) is

$$\eta^S = A\cos(\alpha x) \tag{7}$$

with unknown (complex) amplitude A.

The unknown amplitudes A, B, C may be determined by requiring 1) continuity of surface displacement, 2) continuity of upper-layer cross-shelf mass transport, and 3) vanishing of the cross-shelf velocity in the lower layer of the deep ocean ($u^L = 0$), all at $x = 1$. This leads to three matching conditions at $x = 1$, namely:

$$\eta^S = \eta^D, \tag{8a}$$

$$d\eta_x{}^S = H_1\eta_x{}^D, \tag{8b}$$

$$\eta_{xxx}{}^D + \left(\frac{\omega^2}{\epsilon H_1} - l^2\right)\eta_x{}^D = 0. \tag{8c}$$

Substitution of (4), (5) and (7) into (8) produces three linear equations with three unknowns A, B, C:

$$A\cos\alpha \quad -B \quad -C \quad = \mu^{-1}, \tag{9a}$$

$$A\frac{d}{H_1}\sin\alpha \quad -Bi\beta_- \quad -C\beta_+ \quad = -i\beta_-\mu^{-1}, \tag{9b}$$

$$Bi\beta_-\left(\frac{1}{c_-^2} - \frac{1}{\epsilon H_1}\right) + C\beta_+\left(\frac{1}{c_+^2} - \frac{1}{\epsilon H_1}\right) = i\beta_-\left(\frac{1}{c_-^2} - \frac{1}{\epsilon H_1}\right)\mu^{-1}. \tag{9c}$$

Solutions of (9) may be found for any choice of the five parameters (ϵ, H_1, ω, l, d), provided that α, β_+, β_- are real.

Of primary interest here is the response over the shelf, represented by A, which is expected to be largest near the edge-wave resonances of the unstratified case. These resonances are well known and occur where the following dispersion relation is satisfied (Buchwald and de Szoeke, 1973):

$$\beta_0 = \alpha_0 d\tan\alpha_0, \tag{10}$$

where $\beta_0{}^2 = l_0{}^2 - \omega_0{}^2$ and $\alpha_0{}^2 = (\omega_0{}^2/d) - l_0{}^2$. A typical dispersion diagram is shown in Fig. 2 for $d = \frac{1}{6}$. There is an infinite set of discrete edge-wave modes which occur between the lines $\omega_0 = l_0$ and $\omega_0 = d^{1/2}l_0$. The mode numbers correspond to the number of zero-crossings in the surface elevation over the shelf. A mirror-image picture exists at negative wavenumbers.

A typical example of the response over the shelf to an incident internal wave is shown in Fig. 3 where $|A|$ is plotted versus l for constant frequency $\omega = 2.0$ and $\epsilon = 0.002$, $H_1 = \frac{1}{2}$ and $d = \frac{1}{6}$. The two spikes in the shelf response correspond very nearly to the edge-wave resonances of (10) at $l_0 = 2.44$ and $l_0 = 4.66$ ($\omega_0 = 2.0$). Of course, there can be no perfect resonances in the two-layer model because energy is constantly leaking away from the shelf in the form

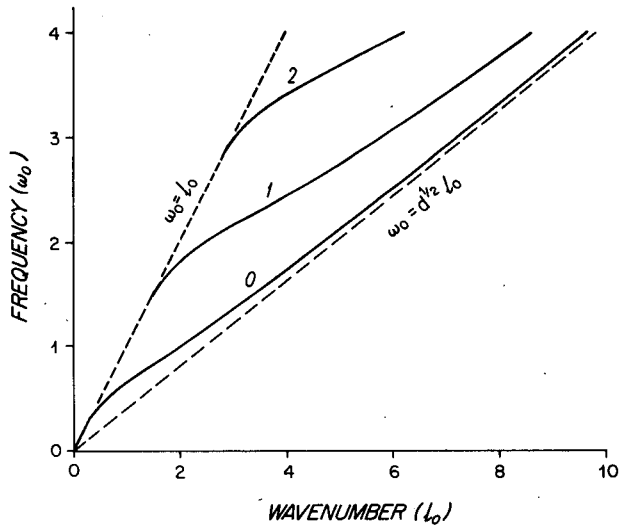

FIG. 2. Dispersion curves for perfectly trapped edge waves over a step shelf, given by (10) with scaled shelf depth $d = \frac{1}{6}$.

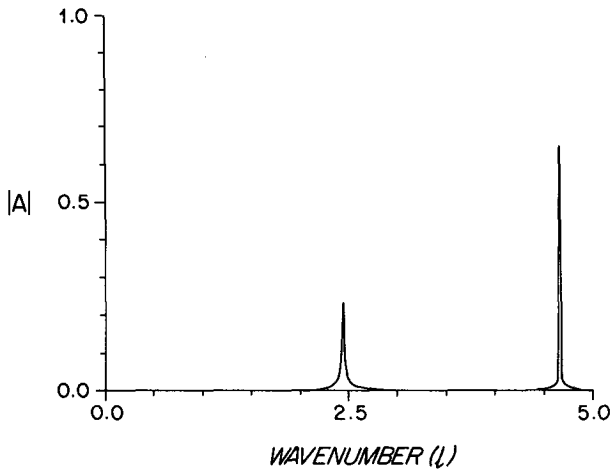

FIG. 3. Surface displacement amplitude over the shelf $|A|$ versus alongshelf wavenumber l for fixed frequency $\omega = 2.0$ and $\epsilon = 0.002$, $H_1 = \frac{1}{2}$, $d = \frac{1}{6}$. Spikes occur near the edge-wave resonances of Fig. 2.

of the reflected internal wave [the second term on the right-hand side of (4)]. Nevertheless, the predicted peak amplitudes are remarkably large, being O(1) quantities. Thus, a unit-amplitude interface displacement can generate (at the resonant peaks) a surface displacement over the shelf of order one, in distinct contrast to the standard $O(\epsilon)$ effect on surface displacement due to an O(1) interface displacement (over a flat bottom). In terms of velocity, this means that an incident upper-layer velocity of $O(\epsilon^{1/2})$ can produce an O(1) velocity over the shelf.

3. Near-resonant response

The only appreciable shelf responses in the entire (ω, l) plane occur near the edge-wave resonances given by (10), so it is appropriate to examine the solutions of (9) near the edge-wave resonances in more detail. To do this, B and C are first eliminated from (9) to obtain an equation for A. For simplicity, $O(\epsilon)$ terms are neglected when compared to O(1) terms. The result is

$$A[\cos\alpha - d\alpha \sin\alpha(\beta_+^{-1} - iH_2/H_1\beta_-)] = -2\epsilon H_2. \tag{11}$$

(The right-hand side is retained because it is the largest term there.) Next, the frequency (or wavenumber) is assumed to be resonant, $\omega = \omega_0$ (or $l = l_0$), while the wavenumber (or frequency) is assumed slightly off resonance $l = l_0 + \Delta l$ (or $\omega = \omega_0 + \Delta\omega$) where $l_0\Delta l \ll 1$ (or $\omega_0\Delta\omega \ll 1$). Keeping only $O(l_0\Delta l)$ or $O(\omega_0\Delta\omega)$ terms leads to

$$A[a\xi + i(b\xi + c)] = -e, \tag{12}$$

where if $\xi = \Delta l$, then

$$a = l_0'\left[\left(\frac{d\alpha_0}{\beta_0^3} + \frac{d}{\alpha_0\beta_0} + \frac{1}{\alpha_0}\right)\sin\alpha_0 + \frac{d}{\beta_0}\cos\alpha_0\right],$$

$$b = -l_0\frac{dH_2}{\omega_0}\left(\frac{\epsilon H_2}{H_1}\right)^{1/2}\left(\frac{\sin\alpha_0}{\alpha_0} + \cos\alpha_0\right),$$

$$c = \frac{H_2}{\omega_0}d\alpha_0\left(\frac{\epsilon H_2}{H_1}\right)^{1/2}\sin\alpha_0,$$

$$e = 2\epsilon H_2,$$

and if $\xi = \Delta\omega$, then

$$a = -\omega_0\left\{\left[\frac{d\alpha_0}{\beta_0^3} + \frac{d\alpha_0}{\omega_0^3}(\epsilon H_1 H_2)^{1/2} + \frac{1}{d\alpha_0} + \frac{1}{\alpha_0\beta_0}\right]\sin\alpha_0 + \frac{\cos\alpha_0}{\beta_0}\right\},$$

$$b = H_2\left(\frac{\epsilon H_2}{H_1}\right)^{1/2}\left(\frac{\sin\alpha_0}{\alpha_0} + \cos\alpha_0\right),$$

$$c = \frac{H_2}{\omega_0}d\alpha_0\left(\frac{\epsilon H_2}{H_1}\right)^{1/2}\sin\alpha_0,$$

$$e = 2\epsilon H_2.$$

The maximum free-surface amplitude over the shelf occurs at $\xi = -bc/(a^2 + b^2)$ which is always within $O(\epsilon)$ of the edge-wave resonance. Thus, the maximum shelf amplitude is (to the same order)

$$|A|_{\max} \approx \frac{e}{c} = \frac{2\omega_0(\epsilon H_1/H_2)^{1/2}}{d\alpha_0 \sin\alpha_0}. \tag{13}$$

The dependence of $|A|_{\max}$ on stratification ϵ and upper-layer thickness H_1 is clear; increasing either quantity increases $|A|_{\max}$. The dependence on ω_0, l_0 and d, however, is tied to the edge-wave dispersion relation (10). A typical example is shown in Fig. 4 where $|A|_{\max}$ from (13) is plotted versus ω_0 following along the dispersion curves of Fig. 2 with $(\epsilon H_1/H_2)^{1/2} = 0.026$ and $d = \frac{1}{6}$. The amplitude is largest at the beginning of each dispersion curve ($\omega_0 \approx l_0$) and then decreases rapidly before beginning a gradual rise as $\omega_0 \to \infty$. It can be shown that $|A|_{\max}$ increases linearly with ω_0 as $\omega_0 \to \infty$. Note that even the minimum values along each curve are much greater than $O(\epsilon)$ and are nearly O(1).

An estimate of the dissipation rate for the edge waves may be obtained by computing the Q of the system, defined as the time-averaged energy stored in the system divided by the energy loss per cycle (which is equivalent to the resonant frequency divided by the bandwidth of the resonant peak at the half-power point). From (12), this results in frequency and wavenumber Q-values given, respectively, by

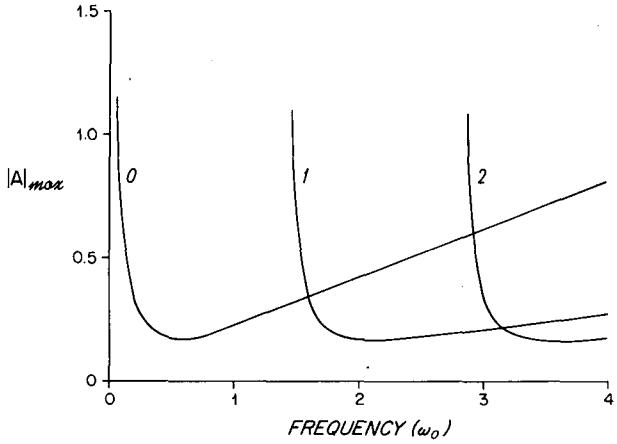

FIG. 4. Maximum surface displacement amplitude over the shelf, $|A|_{\max}$, given by (13), versus frequency ω_0 following along the dispersion curves of Fig. 2. Here $l = l_0$ and is not fixed, $(\epsilon H_1/H_2)^{1/2} = 0.026$ and $d = 1/6$.

$$Q_\omega = \frac{\omega_0 a}{2c}, \quad Q_l = \frac{l_0 a}{2c}, \tag{14}$$

where the appropriate a-values are used. Since c is $O(\epsilon^{1/2})$ while a is O(1), the Q-values are typically quite large (Fig. 5) suggesting that, once excited, the edge waves decay (due to radiation of the reflected internal wave) extremely slowly in both time and space.

From an observational standpoint, $|A|$ may be thought of as the gain of the transfer function between internal waves and edge waves with a power-amplification factor of $|A|^2$ between internal- and edge-wave spectra. If a resonant peak is narrower than the finest experimental resolution (probably a reasonable assumption for such narrow peaks), then the *observable* power-amplification factor is really the integral of $|A|^2$ under the resonant peak (which is proportional to the energy in the peak), given by

$$T_\omega, T_l \approx \int_{-\infty}^{\infty} |A|^2 d\xi = \frac{\pi e^2}{ca}, \tag{15}$$

with the appropriate a-value used. (The infinite limits are used for simplicity because the peak is so narrow.) Figure 6 shows an example of T for the wavenumber resonant peak ($\xi = \Delta l$) following along the dispersion curves of Fig. 2 with $\epsilon = 0.002$, $H_1 = 1/4$ and $d = 1/6$. There is a rapid increase in T along each dispersion curve to a local maximum and then a slow decrease to a constant value as $\omega_0 \to \infty$. Since the maximum peak amplitudes increase as $\omega_0 \to \infty$ (Fig. 4), the peaks themselves must become narrower as $\omega_0 \to \infty$ in order for T to remain constant (Fig. 6). The peaks also become very tall and narrow as $\omega_0 \to 0$. The implications of these results are discussed further in the next section.

With other choices of shelf depth d, the variations of $|A|_{\max}$, T and Q along the dispersion curves are qualitatively identical to those in Figs. 4–6. Generally, as the shelf depth decreases, $|A|_{\max}$ and T tend to increase while Q tends to decrease slightly. However, direct comparisons can be misleading because the dispersion curves change with shelf depth, so that the quantities are not computed for the same (ω_0, l_0) pairs.

4. Summary

The purpose of the model presented here is to demonstrate qualitatively that deep-ocean internal waves may represent a possible energy source for the

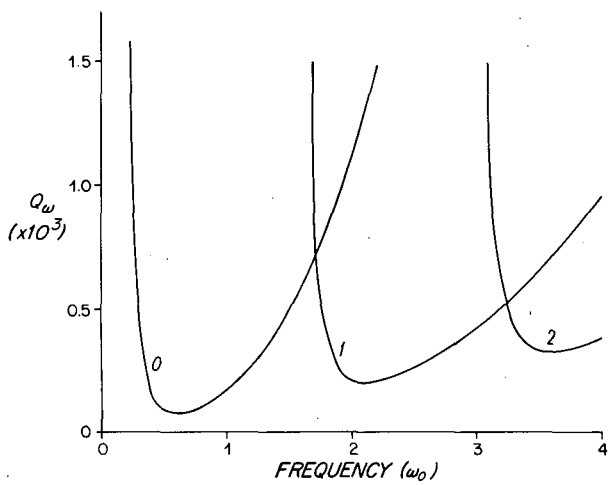

FIG. 5. Plot of Q_ω, given by (14), for the frequency-resonant peaks versus ω_0 following along the dispersion curves of Fig. 2. Here $l = l_0$ and is not fixed, $\epsilon = 0.002$, $H_1 = 1/4$ and $d = 1/6$.

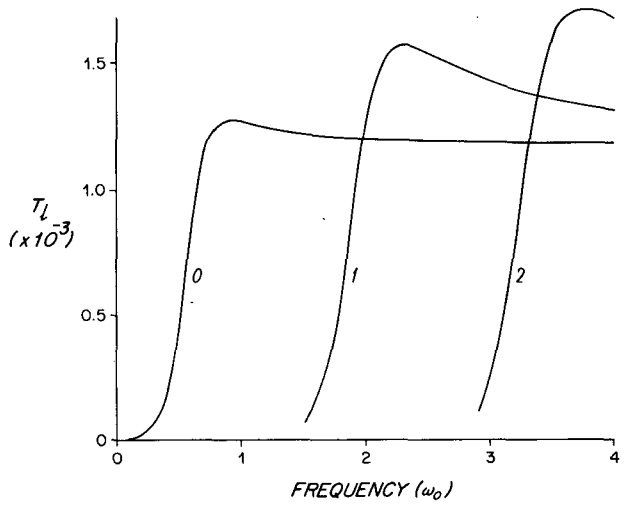

FIG. 6. Integral of $|A|^2$ under the wavenumber-resonant spectral peak T_l given by (15) with $\xi = \Delta l$, versus ω_0 following along the dispersion curves of Fig. 2. Here $l = l_0$ and is not fixed, $\epsilon = 0.002$, $H_1 = 1/4$ and $d = 1/6$.

generation of surface edge-wave "noise" like that observed by Munk *et al.* (1964). Several features of the model results support this hypothesis, the most obvious being that the internal waves can generate edge waves with substantial surface displacements. The present model suggests that the surface displacements of the edge waves may be of the same order of magnitude as the interface displacements (Fig. 4) even with a realistically small density difference between layers ($\epsilon = 0.002$). This is a clear exception to the idea that surface displacements due to interface displacements are typically reduced by the factor ϵ.

Of course, the large amplitudes at the resonant peaks could not be resolved experimentally, so the observable power-amplification factor T should be used to estimate the rms edge-wave amplitude that might be generated by deep-sea internal waves. However, because of the simplified nature of the model, this is, at best, an order-of-magnitude estimate. For example, T_ω for the lowest-mode, frequency-resonant peak levels off at $\sim 4 \times 10^{-4}$ (nondimensional) with increasing frequency. In this range, a deep-sea, internal-wave, vertical-displacement spectral estimate of about 10^3 cm^2 (cph)$^{-1}$ [not unreasonable at frequencies of 2–8 cph (Briscoe, 1975)] leads to an edge-wave spectral estimate of 0.4 cm^2 (cph)$^{-1}$ which is the same order observed by Munk *et al.* (1964). Thus, the power-amplification factor of the model resonant peaks is not inconsistent with the present edge-wave generation mechanism.

Deep-sea internal waves would be expected to represent a fairly constant energy source, but even if the forcing were intermittent, the very high Q-values of the edge waves (Fig. 5) suggest that the waves would persist long after being excited. Either situation is in agreement with the fairly constant edge-wave "noise" observed by Munk *et al.* (1964). Further, the model predicts that the lowest-mode edge wave is most highly excited at low frequencies with mode one becoming comparably (or slightly more) excited at higher frequencies (Fig. 6). Munk *et al.* (1964) also observed this quality; mode zero accounted for 80% of the energy at 4 cph whereas modes zero and one each accounted for 40% of the energy at 7 cph.

From a quantitative standpoint, a number of aspects of the model make it oversimplified and preclude any proper comparison with observations other than order-of-magnitude arguments. For example, the step-shelf topography is not intended to model accurately the Southern California shelf, making direct comparison with observations difficult because dispersion curves for edge waves over more realistic topography will be different from those in Fig. 2. It is for this reason that dimensional frequencies and wavenumbers have not been estimated. A further (and perhaps more damaging) simplification is the simple two-layer stratification for which there is no upper limit to the internal-wave frequency (i.e., the buoyancy frequency is infinite and internal waves may occur at all edge-wave frequencies). A more realistic model with smooth stratification would thus allow the proposed generation mechanism only at frequencies below the buoyancy frequency. Along the Southern California coast, the buoyancy frequency may be as high as 10 cph (Winant and Bratkovich, 1981), which would be high enough to include the edge-wave "noise" emphasized by Munk *et al.* (1964). However, they also observed edge waves at higher frequencies (up to 60 cph but of lesser energy density), which would require some generation mechanism other than deep-sea internal waves. Perhaps there is a transition between forcing by internal waves at low frequencies and by incident surface waves at higher frequencies. This remains to be studied.

The deep pycnocline of the present model (Fig. 1) is also an unrealistic feature. The problem is easily formulated with the interface shallower than the shelf depth ($H_1 < d$). This has been done in the present study (not included here), but the qualitative results are basically unchanged. The problem is more complex because of the internal wave over the shelf whose amplitude is highly sensitive to the choice of parameters, thus quantitatively altering the surface displacement over the shelf. Little appears to be gained from that approach. Another simplification is the neglect of frictional effects (which are difficult to parameterize in a realistic manner). Simple linear friction over the shelf has been added to the model (see the Appendix) with the (expected) result that the spectral peaks and the corresponding Q-values may be substantially reduced by friction. However, this is difficult to put into a realistic context considering the other simplifications. Finally, rotation effects have been neglected, but they were not really observable (Munk *et al.*, 1964) and would only alter the details at very low frequencies.

In conclusion, it appears possible that the surface edge-wave "noise" observed by Munk *et al.* (1964) could have been generated by deep-sea internal waves, but more realistic models must be studied before detailed comparisons with observations can be made.

Acknowledgments. Discussions with K. Brink, W. Munk and M. Hendershott are gratefully acknowledged. I also thank R. Guza for several helpful comments on an earlier version of the manuscript. This research was supported by the National Science Foundation under Grants OCE82-00126 and OCE80-14941.

APPENDIX

Linear Friction Over the Shelf

The model in Section 2 is easily modified to include linear bottom friction over the shelf. Following Buchwald (1980), the terms $-ru$ and $-rv$ are added

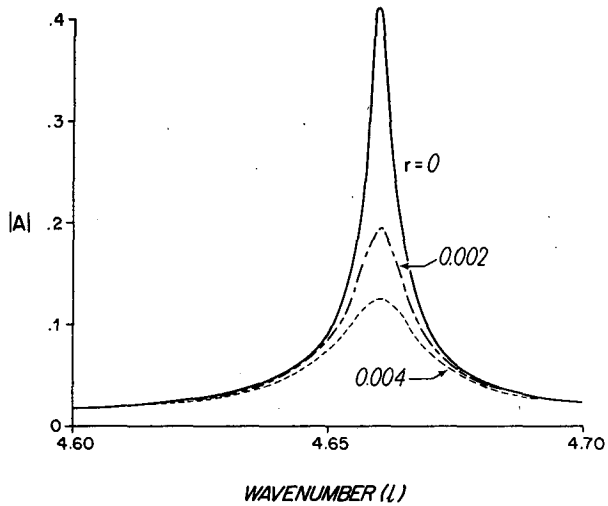

FIG. A1. The effect of linear bottom friction over the shelf on the resonant peak in surface displacement amplitude $|A|$ over the shelf at $\omega_0 = 2.0$ and $l_0 = 4.66$ (mode zero). Here $\epsilon = 0.002$, $H_1 = \frac{1}{2}$, $d = \frac{1}{6}$ and $r = 0.0, 0.002, 0.004$.

to the right-hand side of (1a) and (1b), respectively (when applied to the shelf), where r is the bottom friction coefficient. Using the same scaling as was applied to (1) and (2), r is scaled by $(gH)^{1/2}/L$. The only change in (3)–(8) is that d is replaced by d/F where the friction factor $F = 1 - ir/\omega$ and r/ω is assumed small. Thus, α is defined by

$$\alpha^2 = \frac{\omega^2 F}{d} - l^2, \tag{A1}$$

and the matching condition (8b) now becomes

$$\frac{d}{F}\eta_x^S = H_1\eta_x^D. \tag{A2}$$

The matrix equation (9) is unchanged except for the first term in (9b) which becomes $A(d/H_1F)\sin\alpha$.

With friction over the shelf, there are no perfectly trapped edge waves even in the unstratified case, so that (10) does not apply. However, the maximum response still occurs near the resonances given by (10). Figure A1 shows one such resonant peak (for mode zero) with and without frictional effects. The values used here correspond roughly to depth-averaged shelf friction in the range 0.01–0.2 cm s^{-1} depending on the choice of H, L and shelf depth for scaling. Not surprisingly, the peak is substantially reduced by friction. However, given the other uncertainties in the model (e.g., topography and stratification) it is unclear how to apply these frictional results in a quantitative way.

REFERENCES

Beardsley, R. C., H. Mofjeld, M. Wimbush, C. N. Flagg and J. A. Vermersch, Jr., 1977: Ocean tides and weather-induced bottom pressure fluctuations in the Middle Atlantic Bight. *J. Geophys. Res.*, **82,** 3175–3182.

Bowen, A. J., and R. T. Guza, 1978: Edge waves and surf beat. *J. Geophys. Res.*, **83,** 1913–1920.

Briscoe, M. G., 1975: Preliminary results from the tri-moored internal wave experiment (IWEX). *J. Geophys. Res.*, **80,** 3872–3884.

Buchwald, V. T., 1980: Resonance of Poincaré waves on a continental shelf. *Aust. J. Mar. Freshwater Res.*, **31,** 451–457.

——, and R. A. de Szoeke, 1973: The response of a continental shelf to travelling pressure disturbances. *Aust. J. Mar. Freshwater Res.*, **24,** 143–158.

Cushman-Roisin, B., and J. J. O'Brien, 1983: The influence of bottom topography on baroclinic transports. *J. Phys. Oceanogr.*, **13,** 1600–1611.

Gill, A. E., 1982: *Atmosphere-Ocean Dynamics.* Academic Press, 662 pp.

Huntley, D. A., R. T. Guza and E. B. Thornton, 1981: Field observations of surf beat 1. Progressive edge waves. *J. Geophys. Res.*, **86,** 6451–6466.

Huthnance, J. M., 1975: On trapped waves over a continental shelf. *J. Fluid Mech.*, **69,** 689–704.

Miles, J. W., 1981: A note on edge waves on a flat shelf. *Geophys. Astrophys. Fluid Dyn.*, **18,** 243–251.

Munk, W., F. Snodgrass and G. Carrier, 1956: Edge waves on the continental shelf. *Science,* **123,** 127–132.

——, —— and F. Gilbert, 1964: Long waves on the continental shelf: An experiment to separate trapped and leaky modes. *J. Fluid Mech.*, **20,** 529–554.

Mysak, L. A., 1968: Effects of deep-sea stratification and current on edge waves. *J. Mar. Res.*, **26,** 34–42.

Rattray, M., Jr., 1960: On the coastal generation of internal tides. *Tellus,* **12,** 54–62.

Romea, R. D., and J. S. Allen, 1982: On forced coastal trapped waves at low latitudes in a stratified ocean. *J. Mar. Res.*, **40,** 369–401.

Winant, C. D., and A. W. Bratkovich, 1981: Temperature and currents on the southern California shelf: A description of the variability. *J. Phys. Oceanogr.*, **11,** 71–86.